Catalytic combustion of VOCs on Pt/CuMnCe and Pt/CeY honeycomb monolithic catalysts☆

Anming Zhu, Ying Zhou[**], Yue Wang, Qiulian Zhu, Huayan Liu, Zekai Zhang, Hanfeng Lu[*]

Innovation Team of Air Pollution Control, College of Chemical Engineering, Institute of Catalytic Reaction Engineering, Zhejiang University of Technology, Hangzhou 310014, China

ARTICLE INFO

ABSTRACT

The metal oxides CuMnCe and CeY washcoats on cordierite were prepared using an impregnation method, and then used as support for the active Pt component to prepare the Pt/CuMnCe and Pt/CeY monolithic catalysts for the deep oxidation of VOCs. In comparison with the Pt/CeY, CuMnCe, and CeY monolithic catalysts, the Pt/CuMnCe monolithic catalyst shows an excellent performance for toluene, ethyl acetate, and *n*-hexane oxidation and the $T_{90\%}$ is low to 216, 200 and 260 °C, respectively. The active components Pt/PtO and CuMnCe result in a better synergetic interaction, which promote the catalyst reducibility, increase the oxygen mobility, and enhance the adsorption and activation of organic molecules.

1. Introduction

Environmental problems, especially air pollution is a global concern. Reducing the amount of volatile organic compounds (VOCs) contamination is an important issue for environmental protection.[1] VOCs include a wide range of compounds, such as oxygenates, aromatics, and halogenated hydrocarbons, which can not only destroy the ozone layer, but also cause persistent and cumulative influence on human health and the ecological environment.[2,3] Catalytic combustion is as a potent method of controlling emissions of VOCs due to its high destructive efficiency, low operating cost, and low secondary pollution.[4,5] Hence, developing catalysts with high activity, high universality, and good stability is necessary for VOCs catalytic combustion.

The commonly used catalysts for this application are supported noble metals (mainly Pt and Pd) and transition metal (i.e., Cu, Co, Ce, and Mn) oxides.[6,7] The selection of catalyst depends on a number of factors, such as the nature of the pollutants. Organic air pollutants in industrial exhaust gases are usually mixtures of several compounds with different characteristics. Noble metal or transition metal catalysts cannot effectively oxidize various organic compounds simultaneously at low temperature and may cause secondary pollution to the environment. Researchers showed that Pd and Pt exhibit higher activity toward hydrocarbons and aromatics.[8] The noble metal active sites of Pt/PtO can readily adsorb and activate aromatic hydrocarbon molecules and show high activity, low light-off temperature, and good selectivity to CO_2.[9–11] However, noble metal catalysts are less active for the combustion of oxygenated compounds and cannot be completely oxidized at low temperature. On the contrary, transition metal oxides are more active in the oxidation of oxygenated compounds than noble metals.[3] Among the metal oxides catalysts, copper,[12–14] manganese,[15–18] and their mixed oxides have been widely used in the catalytic combustion of VOCs. Our previous work[18] reveals that the synergy between Cu, Mn, and Ce enhances the catalytic activity; Cu–Mn–Ce ternary oxides can complete the oxidation of various oxygenated compounds under 220 °C. The M–O (e.g. Cu, Ce, Mn, Co) band is the active phase of such metal oxides. Thus, the active oxygen combined with the metal is directly involved in the reaction and easily adsorbs and activates oxygen-containing compounds.[19] However, metal oxide catalysts are less active in the oxidation of aromatic hydrocarbons than noble metals and have undesirable thermal stability.

Noble metal catalysts commonly have a synergistic effect with the transition metal oxide support, due to electron transfer between the noble metal and transition metal oxide.[20–24] A typical example is the Au/TiO₂ catalyst, through the synergy between Au/TiO₂ interface and TiO₂ resulting in efficient oxidation of CO.[20] Researchers showed that other transition metal oxides as a support for the noble metal catalysts can also improve the catalytic activity, such as Au/ZnO,[21] Pt/FeO$_x$,[22] Pd/Fe₃O₄[23] and Ag/MnO$_x$[24] catalysts. Therefore, the "synergy" between the noble metal and the transition metal or the support can not only reduce the cost of catalyst but also improve its catalytic performance.

In addition, due to the high pressure drop of powder catalysts at high flow rates, the implementation of catalysts in industry most widely used is the monolithic catalysts, such as ceramic or metallic honeycomb monoliths.[25,26] In this work, a double-active-site Pt/CuMnCe monolithic catalyst was prepared using an impregnation method, which combined the catalytic merits of noble metal and transition metal catalysts. In comparison with the Pt/CeY, CuMnCe, and CeY monolithic catalysts, the Pt/CuMnCe monolithic catalyst showed higher activities for the combustion of toluene, ethyl acetate and *n*-hexane. This superior activity can be ascribed to the synergy between Pt and CuMnCe, which enhanced the reducibility of the catalyst.

2. Experimental

2.1. Monolithic catalyst preparation

A commercial cylindrical cordierite honeycomb (MgO·Al₂O₃·SiO₂) with 10 mm diameter and 50 mm length was used as the substrate.

A mixed solution of copper nitrate, manganese nitrate, and cerium nitrate dissolved in distilled water was prepared at a molar ratio of 1:2:4. The same moles of citric acid were added into the nitrate solution. The cordierite monolith was immersed in this solution for 1 h. It was dried at 110 °C for 2 h and then calcined at 500 °C in air for 3 h. The monolith washcoated with CuMnCe was labeled as CMC/CH. For comparison, the CeY/monolith was also prepared using the same method by using cerium nitrate and yttrium nitrate at a molar ratio of 4:1. The monolith washcoated with CeY was labeled as CeY/CH. The contents of the CuMnCe and CeY washcoats were approximately 3.6 wt%–3.9 wt% in the CuMnCe/monolith and CeY/monolith.

The Pt supported on the CuMnCe/monolith, designated Pt/CMC/CH catalyst, was impregnated with 10 mL aqueous solution of H₂PtCl₆·6H₂O at a concentration of 0.2 g/L. Then the catalyst was dried at 110 °C for 2 h and calcined at 500 °C for 3 h. The Pt/CeY/monolith was also prepared using the same method and was designated Pt/CeY/CH. The content of Pt was approximately 0.02 wt% in the Pt/CMC/CH and Pt/CeY/CH.

2.2. Powder catalyst preparation

A mixed solution of copper nitrate, manganese nitrate, and cerium nitrate dissolved in distilled water was prepared at a molar ratio of 1:2:4. Then citric acid equimolar to the metal nitrates was added to the nitrate solution. The resulting solution was stirred and dried, and then calcined at 500 °C for 3 h. For comparison, the CeY mixed oxide was also prepared using the same method.

The CuMnCe mixed oxide was impregnated with an aqueous solution of H₂PtCl₆·6H₂O to control Pt loading at 0.02 wt%. After stirring, the catalyst was dried at 110 °C for 2 h and calcined at 500 °C for 3 h. The Pt/CeY powder catalyst was also prepared using the same method.

2.3. Catalyst characterization

The scanning electron microscopy (SEM) characterization was carried out on a HitachiS-4700 II apparatus to get the surface profile of the samples.

Transmission electron microscopic (TEM) images of the catalysts were obtained on a FEI Tecnai G2 F30 S-Twin apparatus operated at 300 kV. The energy dispersive X-ray (EDX) analysis was used to record elemental composition in a selected area of the specimen.

X-ray diffraction (XRD) patterns were collected in a 2θ range from 10° to 100° with a step interval 0.02° on an ARLSCINTAG X'TRA powder diffractometer.

H₂-temperature programmed reduction (H₂-TPR) was tested on an Autochem 3010E (Zhejiang Fine-Tech Instruments, China). A desired amount of sample (100 mg) was placed in a quartz reactor, pretreated in a flow of Ar gas at 200 °C for 2 h, and cooled to 50 °C. A gas mixture of H₂ (5%) and Ar (95%) was then passed (30 mL/min) through the reactor. The temperature was increased from 50 °C to 900 °C at a heating rate of 10 °C/min. A TCD detector was used at the outlet of the reactor to measure the volume of hydrogen consumed during reduction.

The residual Pt content was determined using a UV-2600 spectrograph by following the external standard method. The actual Pt content was calculated using Eq. (1) as follows:

$$\Delta w_{Pt} = \frac{(0.2 - C_{Pt}) \times 0.01}{m_{monolith}} \qquad (1)$$

where, C_{Pt} represents the concentration of residual Pt; $m_{monolith}$ represents the weight of the monolithic catalyst after loading Pt.

The cohesive ability of the active phase on the cordierite honeycomb was performed by an ultrasonic vibration cleaner. The samples were subjected to ultrasonic cleaning by being immersed in water inside a glass vessel. After ultrasonic cleaning for 30 min at 40 kHz, the samples were dried, calcinated, and weighed.

2.4. Catalytic experiments

Catalytic reaction was conducted in a fixed-bed quartz tube reactor with an inner diameter of 17 mm. The concentration of VOCs in air was 2000 ppm and the gas hourly space velocity (GHSV) was 5000 h^{-1}. The conversion of VOCs was analyzed using an online GC 1620 gas chromatograph equipped with an FID detector. Moreover, the reaction by-products and the selectivity of CO₂ of different catalysts were identified using GC-MS analysis during the light-off tests.

3. Results and discussion

3.1. Pt/CMC and Pt/CeY washcoat characterization

The cohesive ability of the washcoat on the substrate is an important criterion for the life of monolithic catalysts. An ultrasonic test was employed to test adherence. The weight losses of the monolithic catalysts are listed in Table 1. The mass losses of all the oxide catalysts are less than 0.5 wt%. This result indicates that the active phase firmly anchored onto the substrate and has tight inosculation with the substrate. The EDX pattern is demonstrated in Table 1 and Fig. 1. For the Pt/CMC/CH catalyst, the surface ratio of the metal ion is proportional to that of the dipping solution. This result is consistent with our previous study that the metal ions in the solution are non selectively adsorbed onto the cordierite surface.[18] However, for the Pt/CeY/CH catalyst, the surface ratio of the

Table 1
Physical–chemical analysis of the Pt/CMC and Pt/CeY monolithic catalysts.

Catalyst	$\Delta\omega$ (%)	Pt content[a] (wt%)	Analyte	Surface ion content of compounds (at%)
Pt/CMC/CH	0.27	0.023	Cu	14.58
			Mn	26.37
			Ce	57.84
			Pt	1.2
Pt/CeY/CH	0.23	0.024	Ce	68.92
			Y	28.75
			Pt	2.31

[a] The content of Pt compared with the weight of monolithic catalyst.
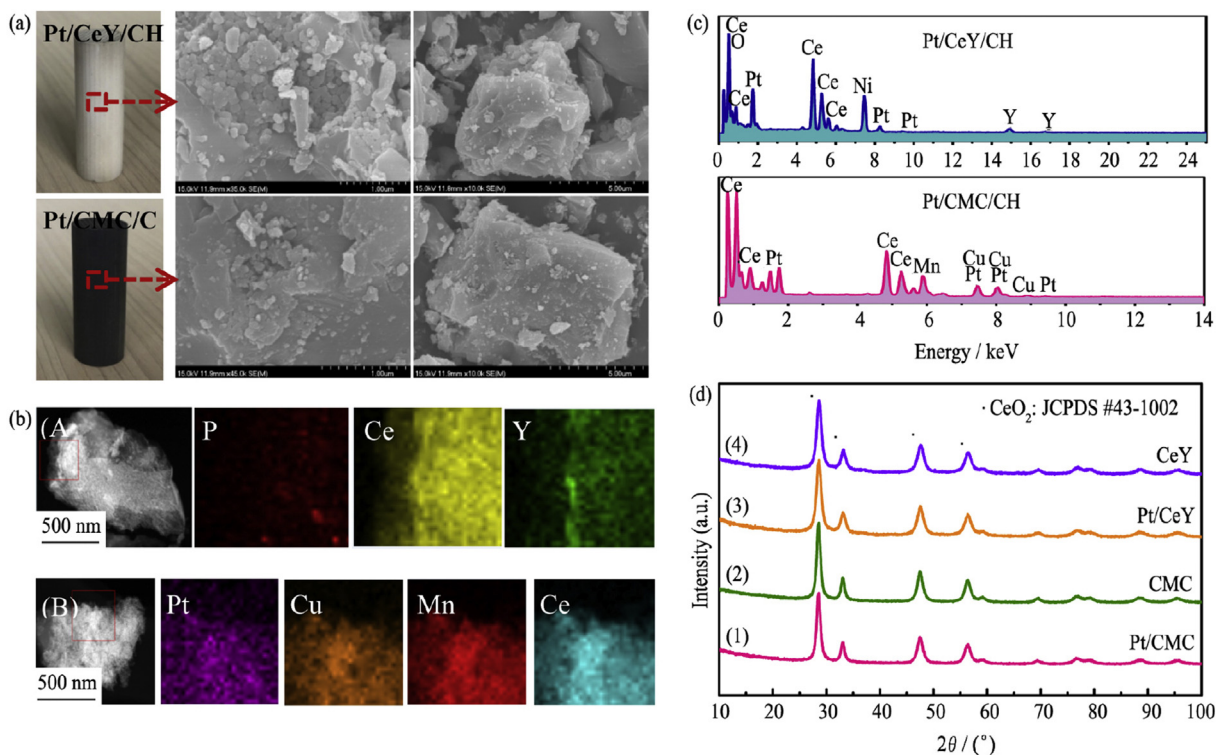

Fig. 1. (a) Photos and SEM images of the Pt/CeY/CH and Pt/CMC/CH catalysts; (b, c) TEM images and EDX spectra of the Pt/CeY/CH (A) and Pt/CMC/CH (B) catalysts; (d) XRD patterns of Pt/CMC (1), CMC (2), Pt/CeY (3), CeY (4) powder catalysts.
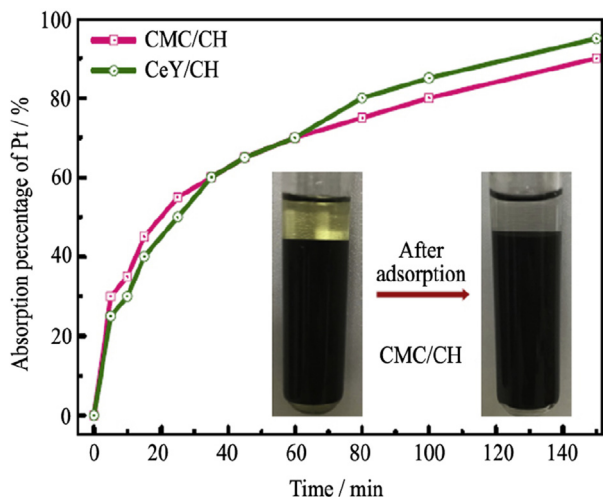

Fig. 2. The adsorption performance of $H_2PtCl_6 \cdot 6H_2O$ for the CMC and CeY washcoats (constant temperature water-bath: 70 °C, time: 150 min).
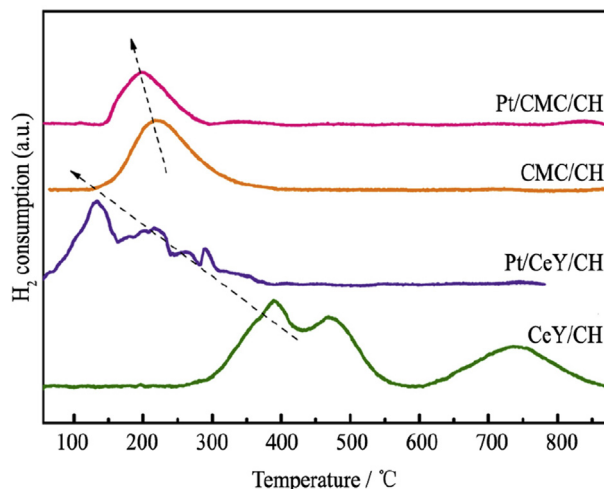

Fig. 3. H_2-TPR profiles of Pt/CMC/CH, Pt/CeY/CH, CMC/CH, and CeY/CH catalysts.

metal ions are 68.72 and 28.75, respectively. This result indicates that the Y ions preferably adhered to the cordierite than the Ce ions.

The adsorption performance of $H_2PtCl_6 \cdot 6H_2O$ for the CMC and CeY washcoats must be taken into account in practical applications. As is shown in Fig. 2, at 60 min, the adsorption quantity of CMC and CeY washcoats reaches 70%. After 150 min, the adsorptive capacity is more than 90% and no washcoat is dissolved during the impregnation. This outcome indicates the strong interaction between the metal ions and cordierite support.

3.2. Structure and texture properties of the catalysts

The appearance of the supported Pt and mixed oxides catalysts is shown in Fig. 1. As can be seen in the figure, a uniform catalytic layer of mixed oxides covering the substrate is formed. The SEM images of the Pt/CMC/CH and Pt/CeY/CH catalysts show that the metal oxide particles aggregated in clusters of different sizes and geometry and adhered to the cordierite surface. The TEM images show that the metal ions of Pt/CMC/CH and Pt/CeY/CH catalysts uniformly distributed on the substrate surface. This uniform distribution facilitates the dispersion of the active phase and the improvement of the catalytic activity.

To eliminate the interference of the strong diffraction peak of the cordierite, XRD patterns were prepared using the Pt/CMC, Pt/CeY, CMC, and CeY powder catalysts. As shown in Fig. 1, the main peaks between 10° and 100° are consistent with the cubic ceria phase (c-CeO$_2$, fluorite-like structure of CeO$_2$ at 28.8°, 33.4°, 47.6°, and 56.6°, JCPDS 43-1002).[2] The diffraction peaks of PtO, CuO$_x$,
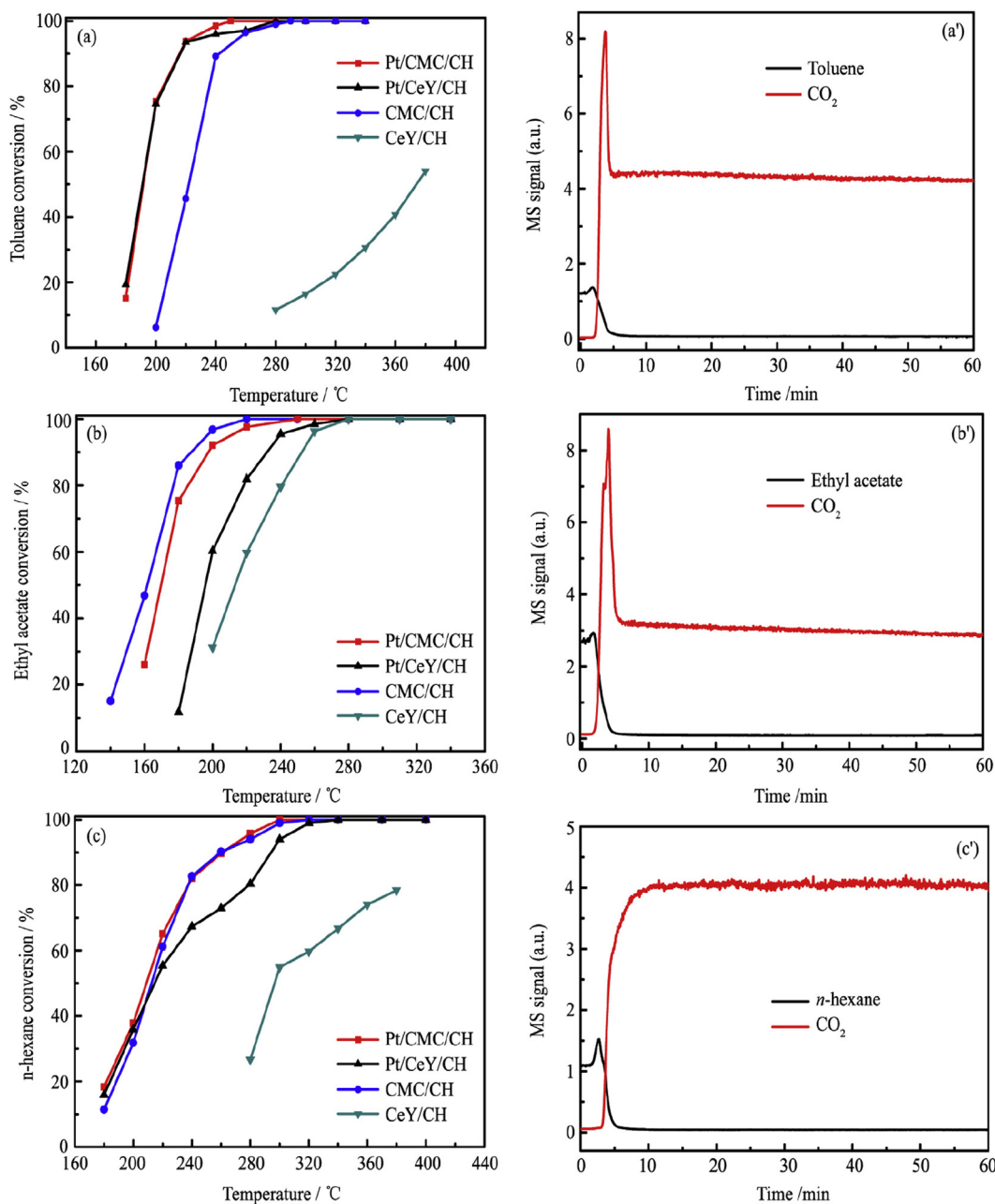

Fig. 4. Light-off curves of toluene (a), ethyl acetate (b) and n-hexane (c) catalytic combustion over the different monolithic catalysts; MS tested curves over the Pt/CMC/CH catalytic oxidation of toluene (a′), ethyl acetate (b′) and n-hexane (c′) (from room temperature to complete oxidation temperature at 3.5 °C/s).

MnO_x, and YO_x are not detected. This result indicates that a ceria-based solid solution structure was formed by the doping of Cu, Mn, and Y ions.[26–28] The noble metal Pt and excess Cu, Mn, and Y are highly dispersed on the surface of CeO_2 as oxides or their mixed oxides.[29] According to available reports,[30,31] the mixed structure of Cu, Mn oxides, and PtO disperses on the surface of the ceria-based solid solution with the function of activating organic molecules and transporting active oxygen.

3.3. Redox properties of the catalysts

To investigate the influence of doping Pt on the redox properties of metal oxides, the H_2-TPR profiles of the different catalysts were investigated and are shown in Fig. 3. The Pt/CMC/CH and CMC/CH catalysts show two peaks centered at about 200 and 225 °C, which can be assigned to the reduction of the surface oxygen of ceria.[29] The peaks also indicated that Ce was partially substituted for Mn, and Cu formed an excellent ceria-based solid solution structure. For the CeY/CH catalyst, three peaks appear centered at about 390, 470, and 750 °C. The peak at 470 °C can be assigned to the reduction of surface CeO_2, and the peak at 390 °C is possibly due to a further reduction of Ce^{4+}. The high temperature peak at 750 °C can be attributed to the reduction of bulk CeO_2 to Ce_2O_3.[28,29,31] In comparison with the CeY/CH catalyst, the redox capacity of CMC/CH is significantly improved, which can be assigned to the presence of such a mixed structure of $Cu_{1.5}Mn_{1.5}O_4$ and CeO_x over Cu–Mn–Ce-based catalysts.[32] The addition of Pt promotes the reduction of surface CeO_2. This effect can be ascribed to the hydrogen spillover from the Pt particles onto the CuMnCe and CeY mixed oxides. Furthermore, the presence of ceria enhances the reduction of platinum particles. This mutual interaction leads to the excellent reactivity of mixed oxides for the oxidation of volatile organics.[31]

3.4. Catalytic activities

The conversion of VOCs as a function of reaction temperature over the different monolithic catalysts is shown in Fig. 4(a–c). The $T_{50\%}$ for the Pt/CMC/CH catalyst is low to 200 °C. A lower $T_{50\%}$ temperature probably means less formation of by-products.[8] In comparison with the Pt/CeY/CH, CMC/CH, and CeY/CH catalysts, the Pt/CuMnCe/CH catalyst shows an excellent performance for toluene, ethyl acetate, and n-hexane oxidation with $T_{90\%}$ is low to 216, 200, and 260 °C, respectively. Their excellent activity can be reasonably attributed to the synergy between Pt and CuMnCe. Many researchers show that the kinetics of the oxidation of VOCs (toluene, ethyl acetate and n-hexane) over Pt/CMC/CH can be expressed using the MVK model.[33–35] Organic molecules are readily adsorbed on Pt surface, and Pt and Cu–Mn mixed structure are the main active site as oxydehydrogenation center, especially the noble metal Pt has strong activation ability of C–H band. The adsorbed VOCs react with oxygen on the catalyst surface, resulting in the reduction of oxygen vacancies.[19] However, the ceria-based solid solution structure with the function of storage and transporting active oxygen (surface and lattice oxygen) can provide sufficient lattice oxygen to further active VOCs. Moreover, the hydrogen spillover from the Pt particles onto the CuMnCe mixed oxides can also promote the activation of VOCs.

To discover the by-products and measure the selectivity of CO_2, all the organic compounds formed during the light-off tests over the different catalysts were analyzed using MS (shown in Fig. 4(a′–c′)). As expected, the formation of organic by-products is not observed during the toluene, ethyl acetate, and n-hexane oxidation. The MS results show that the CO_2 selectivity is very high, and the ignition curve can be represented by following either the
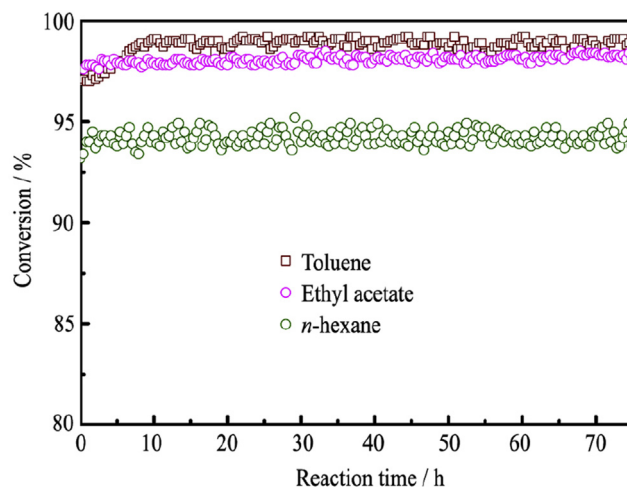

Fig. 5. Durability of the Pt/CMC/CH catalyst for the oxidation of toluene, ethyl acetate, and n-hexane at 240, 220, and 300 °C, respectively.

decrease of the VOCs signal or the increase of the CO_2 signal.[36] Moreover, prolonged catalytic tests were conducted for toluene, ethyl acetate, and n-hexane combustion over Pt/CMC/CH. As shown in Fig. 5, an excellent catalytic activity is observed during the reaction and no obvious deactivation occurs. This result suggests good stability of the catalyst for industrial use.

4. Conclusions

The Pt/CuMnCe monolithic catalyst with double active sites Pt and Cu–Mn–Ce were prepared using a simple impregnation method and used for the catalytic removal of VOCs. The impregnated phases show excellent adhesion to the monoliths. In comparison with the Pt/CeY/CH, CMC/CH, and CeY/CH catalysts, the Pt/CuMnCe/CH catalyst displays good catalytic performance in the oxidation of oxygen-free and oxygenated compounds. This superior activity can be ascribed to the formation of a ceria-based solid solution, the highly dispersed Pt and CuMnCe mixed oxides, and the synergy between Pt and CuMnCe, which enhances the reducibility of the catalyst.

References

1. Topka P, Klementová M. Total oxidation of ethanol over $Au/Ce_{0.5}Zr_{0.5}O_2$ cordierite monolithic catalysts. *Appl Catal A*. 2016;522:130.
2. Shi ZN, Yang P, Tao F, Zhou RX. New insight into the structure of CeO_2-TiO_2, mixed oxides and their excellent catalytic performances for 1,2-dichloroethane oxidation. *Chem Eng J*. 2016;295:99.
3. Su XW, Jin LY, Lu JQ, Luo MF. $Pd/Ce_{0.9}Cu_{0.1}O_{1.9}$-$Y_2O_3$ catalysts for catalytic combustion of toluene and ethyl acetate. *J Ind Eng Chem*. 2009;15(5):683.
4. Azalim S, Brahmi R, Agunaou M, Beaurain A, Giraudon JM. Washcoating of cordierite honeycomb with Ce-Zr-Mn mixed oxides for VOCs catalytic oxidation. *Chem Eng J*. 2013;223:536.
5. Tang WX, Wu XF, Li SD, Li WH, Chen YF. Porous Mn-Co mixed oxide nanorod as a novel catalyst with enhanced catalytic activity for removal of VOCs. *Catal Commun*. 2014;56(2):134.
6. Zhang X, Wu DF. Ceramic monolith supported Mn-Ce-M ternary mixed-oxide (M=Cu, Ni or Co) catalyst for VOCs catalytic oxidation. *Ceram Int*. 2016;42(15):16563.
7. Abdelouahab-Reddam Z, Mail RE, Coloma F. Platinum supported on highly-dispersed ceria on activated carbon for the total oxidation of VOCs. *Appl Catal A*. 2015;94:87.
8. Ojala S. *Catalytic Oxidation of Volatile Organic Compounds and Malodorous Organic Compounds*. University of Oulu; 2005.
9. Wang C, Vliet DVD, Chang KC, You H, Strmcnik D, Schlueter JA, et al. Monodisperse Pt_3Co nanoparticles as a catalyst for the oxygen reduction reaction: size-dependent activity. *J Phys Chem C*. 2009;113(45):19365.
10. Zhou WP, Lewera A, Larsen R. Size effects in electronic and catalytic properties of unsupported palladium nanoparticles in electrooxidation of formic acid. *J Phys Chem B*. 2006;110(27):13393.

11. Nesselberger M, Ashton S, Meier JC, Katsounaros I, Mayrhofer KJJ, Arenz M. The particle size effect on the oxygen reduction reaction activity of Pt catalysts: influence of electrolyte and relation to single crystal models. *J Am Chem Soc*. 2011;133(43):17428.

12. Yang YX, Xu XL, Sun KP. Catalytic combustion of ethyl acetate on supported copper oxide catalysts. *J Hazard Mater*. 2007;139(1):140.

13. Tsoncheva T, Issa G, Blasco T, Dimitrov M, Popova M, Hernández S, et al. Catalytic VOCs elimination over copper and cerium oxide modified mesoporous SBA-15 silica. *Appl Catal A*. 2013;453(6):1.

14. Larsson PO, Andersson A. Oxides of copper, ceria promoted copper, manganese and copper manganese on Al_2O_3, for the combustion of CO, ethyl acetate and ethanol. *Appl Catal B*. 2000;24(3–4):175.

15. Rao T, Shen MQ, Jia LW, Hao JJ, Wang J. Oxidation of ethanol over Mn-Ce-O and Mn-Ce-Zr-O complex compounds synthesized by sol-gel method. *Catal Commun*. 2007;8(11):1743.

16. Sang CK, Wang GS. Catalytic combustion of VOCs over a series of manganese oxide catalysts. *Appl Catal B*. 2010;98(3):180.

17. Esteban CL, Andrs PM, Jorge S, Horacio T. Cerium, manganese and cerium/manganese ceramic monolithic catalysts. Study of VOCs and PM removal. *J Rare Earths*. 2016;34(7):675.

18. Lu HF, Zhou Y, Huang HF, Zhang B, Chen YF. In-situ synthesis of monolithic Cu-Mn-Ce/cordierite catalysts towards VOCs combustion. *J Rare Earths*. 2011;29(9):855.

19. Huang H, Xu Y, Feng Q, Leung DYC. Low temperature catalytic oxidation of volatile organic compounds: a review. *Catal Sci Technol*. 2015;5(5):2649.

20. Green IX, Tang W, Neurock M, Yates Jr JT. Spectroscopic observation of dual catalytic sites during oxidation of CO on a Au/TiO_2 catalyst. *Science*. 2011;333(6043):736.

21. Li P, Wei Z, Wu T, Peng Q, Li YD. Au-ZnO hybrid nanopyramids and their photocatalytic properties. *J Am Chem Soc*. 2011;133(15):5660.

22. Qiao BT, Wang AQ, Yang XF, Allard LF, Jiang Z, Cui YT, et al. Single-atom catalysis of CO oxidation using Pt_1/FeO_x. *Nat Chem*. 2011;3(8):634.

23. Chen S, Si R, Taylor E, Janzen J, Chen J. Synthesis of Pd/Fe_3O_4 hybrid nanocatalysts with controllable interface and enhanced catalytic activities for CO oxidation. *J Phys Chem C*. 2012;116(23):12969.

24. Huang ZW, Gu X, Cao QQ, Hu PP, Hao JM, Li JH, et al. Catalytically active single-atom sites fabricated from silver particles. *Angew Chem Int Ed*. 2012;51(17):4198.

25. Avila P, Montes M, Miró EE. Monolithic reactors for environmental applications: a review on preparation technologies. *Chem Eng J*. 2005;109(1):11.

26. Liang Q, Wu XD, Weng D, Xu HB. Oxygen activation on Cu/Mn-Ce mixed oxides and the role in diesel soot oxidation. *Catal Today*. 2008;139(1–2):113.

27. Tang XF, Xu YD, Shen WJ. Promoting effect of copper on the catalytic activity of MnO_x-CeO_2 mixed oxide for complete oxidation of benzene. *Chem Eng J*. 2008;144(2):175.

28. Luo MF, He M, Xie YL, Fang P, Jin LY. Toluene oxidation on Pd catalysts supported by CeO_2-Y_2O_3, washcoated cordierite honeycomb. *Appl Catal B*. 2007;69(3–4):213.

29. Lu HF, Kong XX, Huang HF, Zhou Y, Chen YF. Cu-Mn-Ce ternary mixed-oxide catalysts for catalytic combustion of toluene. *J Environ Sci*. 2015;32(6):102.

30. Matějová L, Topka P, Kaluža L, Pikäaho S, Ojala S, Gaalova J, et al. Total oxidation of dichloromethane and ethanol over ceria-zirconia mixed oxide supported platinum and gold catalysts. *Appl Catal B*. 2013;142(10):54.

31. Abbasi Z, Haghighi M, Fatehifar E, Saedy S. Synthesis and physicochemical characterizations of nanostructured Pt/Al_2O_3-CeO_2, catalysts for total oxidation of VOCs. *J Hazard Mater*. 2011;186(2–3):1445.

32. Morales MR, Barbero BP, Cadús LE. Total oxidation of ethanol and propane over Mn-Cu mixed oxide catalysts. *Appl Catal B*. 2006;67(3–4):229.

33. Behar S, Gómez-Mendoza NA, Gómez-García MÁ, Świerczyński D, Quignard F, Tanchoux N. Study and modelling of kinetics of the oxidation of VOC catalyzed by nanosized Cu-Mn spinels prepared via an alginate route. *Appl Catal A*. 2015;504:203.

34. Ordóñez S, Bello L, Sastre H, Rosal R, Diez FV. Kinetics of the deep oxidation of benzene, toluene, n-hexane and their binary mixtures over a platinum on γ-alumina catalyst. *Appl Catal B*. 2002;38(2):139.

35. Özçelik TG, Alpay E, Atalay S. Kinetic study of combustion of isopropanol and ethyl acetate on monolith-supported CeO_2 catalyst. *Prog React Kinet Mech*. 2013;38(1):62.

36. Burgos N, Paulis M, Antxustegi MM, Montes M. Deep oxidation of VOC mixtures with platinum supported on Al_2O_3/Al monoliths. *Appl Catal B*. 2002;38(4):251.